

## Autonomous Silva–Young Type Chaotic Oscillator with Flat Power Spectrum

**E. Tamaseviciute**

*Department of Mechanical and Process Engineering, Swiss Federal Institute of Technology in Zürich, CH-8092, Switzerland, phone: +41 7990 37076, e-mail: elenata@student.ethz.ch*

**G. Mykolaitis**

*Department of Physics, Vilnius Gediminas Technical University, Saulėtekio av. 11, LT-10223 Vilnius, Lithuania, phone: +370 5 2619589, e-mail: gytis@pfi.lt*

**A. Tamasevicius**

*Division of Electronics, Center for Physical Sciences and Technology, A. Goštauto str. 11, LT-01108 Vilnius, Lithuania, phone: +370 5 2619589, e-mail: tamasev@pfi.lt*

**crossref** <http://dx.doi.org/10.5755/j01.eee.115.9.761>

### Introduction

Chaotic oscillations have been observed and intensively investigated in a variety of nonlinear electrical circuits [1, 2]. In contrast to common noise originated from random fluctuations, chaos is generated by purely deterministic systems, similar to the periodic waveform oscillators. Therefore chaotic oscillators are notable for their high power and high efficient performance. Unlikely to periodic oscillations characterized by discrete spectra, chaotic oscillations exhibit broadband continuous power spectra. The fields of practical engineering application of chaotic oscillators include, for example, spread spectrum communication systems, information scrambling for secure transmission, also noise radar systems.

Chaotic oscillations can be generated in the third-order or higher-order autonomous nonlinear electrical circuits, for example oscillators described in [3–13]. In the case of non-autonomous circuits, i.e. nonlinear damped oscillators driven by external periodic voltage, the minimal order of the circuit can be reduced to two. However, most of chaotic circuits designed so far have noticeable unevenness of the spectral density. This undesirable feature is observed not only in the non-autonomous second-order nonlinear circuits, but also in the autonomous third-order [3–7], in the fourth-order [8–11] chaotic, in the sixth-order [12] and in higher-order [13] hyperchaotic oscillators.

Using the well-known in nonlinear dynamics the second-order nonlinear Duffing–Holmes equations [14]

$$\begin{cases} \frac{dx}{dt} = y, \\ \frac{dy}{dt} = x - x^3 - by + a \sin \omega_f t. \end{cases} \quad (1)$$

Silva and Young [15, 16] invented a non-autonomous electronic circuit generating chaotic oscillations with a broadband noise-like spectrum. Later Kandangath *et al.* described low-frequency version of the oscillator [17]. A simplified Silva–Young oscillator [18] was used in various physical experiments demonstrating the performance of electronic analogue controllers designed for stabilizing dynamical systems [19, 20]. The main shortcoming of the nonautonomous chaotic oscillators in many practical applications is that they have sharp 20–30 dB height peaks at the external drive frequency  $f_1 = \omega/2\pi$  and its higher harmonics [15]. To get around the problem Lindberg *et al.* recently suggested the third-order autonomous Duffing–Holmes (or Silva–Young) type chaotic oscillator [21] described by the following set of equations:

$$\begin{cases} \frac{dx}{dt} = y, \\ \frac{dy}{dt} = x - x^3 + by - kz, \\ \frac{dz}{dt} = \omega_f(y - z), \end{cases} \quad (2)$$

where  $\omega_f$  is the cut-off frequency of the low-pass RC filter inserted in the negative feedback loop of the oscillator. Though sharp peaks are avoided in the power spectrum, the spectral density still exhibits large undesirable unevenness of about 10–15 dB [21, 22].

In this paper, we describe both, experimentally and numerically the fourth-order nonlinear circuit exhibiting unusually (for deterministic chaotic oscillators) flat power spectrum. In contrast to the Lindberg's [21] chaotic oscillator the novel oscillator includes an additional LC resonant tank in the positive feedback loop.

## Electronic circuitry

The novel fourth-order autonomous circuit is presented in Fig. 1.

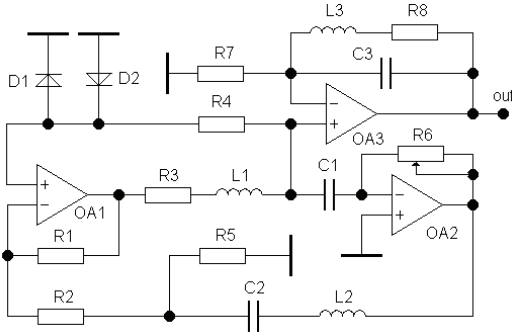


**Fig. 1.** Circuit diagram of the fourth-order autonomous Silva-Young type oscillator

The oscillator comprises an OA1 based nonlinear resonant stage with the diodes D1, D2, the  $L_1C_1$  tank, and resistor  $R_4$  in the first positive feedback loop, also an OA2 based linear resonant stage with the  $L_2C_2$  tank and the load resistor  $R_5$  in the second positive feedback loop. The OA3 based stage is an external output follower with the spectral correction circuit  $L_3R_8C_3$ .

## Experimental results

The typical output signal and the corresponding power spectrum are shown in Fig. 2 and Fig. 3, respectively. The following element values have been used in the experiment:  $L_1=L_2=20$  mH,  $L_3=16$  mH,  $C_1=47$  nF,  $C_2=56$  nF,  $C_3=175$  nF,  $R_1=R_2=20$  k $\Omega$ ,  $R_3=R_8=62$   $\Omega$ ,  $R_4=68$  k $\Omega$ ,  $R_5=100$   $\Omega$ ,  $R_6$ —tuneable,  $R_7=1.5$  k $\Omega$ . The OA1, OA2 and OA3 are the OP-07 type or similar operational amplifiers; the diodes D1 and D2 are the 1N4148 type or similar general-purpose devices.

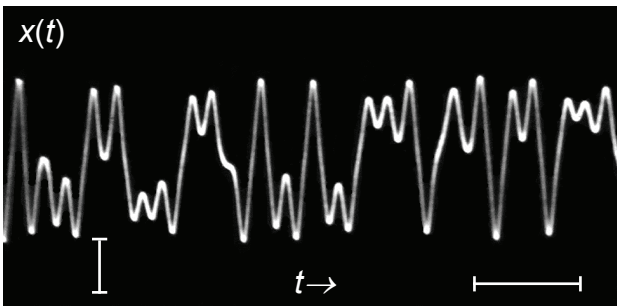


**Fig. 2.** Experimental snapshot of chaotic output waveform. Vertical scale 1 V/div. Horizontal scale 1 ms/div.  $R_6=490$   $\Omega$

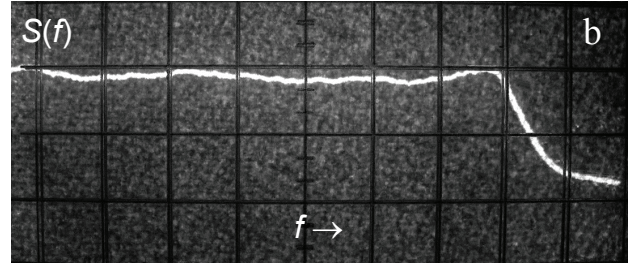
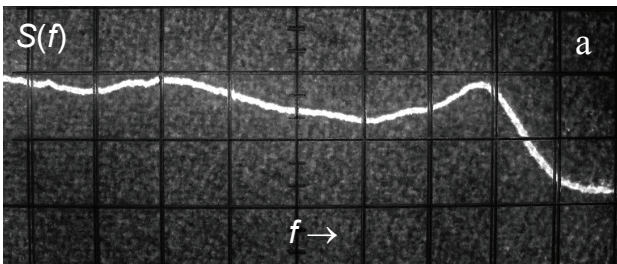


**Fig. 3.** Experimental spectra  $S(f)$  from the output signal  $V_{C1}(t)$ . Vertical scale 10 dB/div., horizontal scale 0.5 kHz/div. Spectral range from 250 Hz to 5 kHz, resolution 100 Hz. (a) without correction (capacitor  $C_3$  short-circuited; gain 0 dB). (b) with correction (resonant gain 6 dB at 3 kHz).  $R_6=490$   $\Omega$

## Equations

Using the Kirchoff's laws the following set of differential equations for the circuit in Fig. 1 is derived:

$$\begin{cases} C_1 \frac{dV_{C1}}{dt} = I_{L1}, \\ L_1 \frac{dI_{L1}}{dt} = kV_D(V_{C1}) - V_{C1} - (R_3 + r_1)I_{L1} + (k-1)R_5I_{L2}, \\ C_2 \frac{dV_{C2}}{dt} = I_{L2}, \\ L_2 \frac{dI_{L2}}{dt} = R_6I_{L1} - V_{C2} - (R_5 + r_2)I_{L2}, \end{cases} \quad (3)$$

where the  $V_{C1}$  and  $V_{C2}$  are the voltages across the capacitor  $C_1$  and  $C_2$ , the  $I_{L1}$  and  $I_{L2}$  are the currents through the inductor  $L_1$  and  $L_2$ , respectively. The  $k$  is the gain of OA1 based stage with respect to the non-inverting input. The  $V_D(V_{C1})$  is the voltage across the diodes  $D_1$  and  $D_2$ , depending on the voltage  $V_{C1}$ , applied via resistor  $R_4$ , and on the state of the diodes (either OFF, or ON). The  $r_1$  and  $r_2$  are the internal resistances of the inductive coil  $L_1$  and  $L_2$ , respectively (specifically,  $r_1=r_2=2$   $\Omega$ ). Other notations are evident from the circuit diagram in Fig. 1. Equations for the correction circuit  $L_3R_8C_3$  are rather trivial and are not presented here for simplicity. Moreover, the OA3 based stage is an external unit used for correction only, i.e. it is not involved in the generation of chaotic oscillations.

Let us introduce a set of the dimensionless state variables  $x, y, z, v$ , dimensionless time  $g$  and parameters  $a, b, c, d, k, \varepsilon, \mu, \rho, \tau$  are given:  $x = \frac{V_{C1}}{2V^*}$ ,  $y = \frac{\rho I_{L1}}{2V^*}$ ,  $z = \frac{V_{C2}}{2V^*}$ ,  $v = \frac{\rho I_{L2}}{2V^*}$ ,  $g = \frac{t}{\tau}$ ,  $\tau = \sqrt{L_1C_1}$ ,  $\rho = \sqrt{\frac{L_1}{C_1}}$ ,  $a = \frac{R_6}{\rho}$ ,  $b = \frac{R_3 + r_1}{\rho}$ ,  $c = (k-1)\frac{R_5}{\rho}$ ,  $d = \frac{R_5 + r_2}{\rho}$ ,  $k = \frac{R_1}{R_2 + R_5} + 1$ ,  $\varepsilon = \frac{C_2}{C_1}$ ,  $\mu = \frac{L_2}{L_1}$  ( $V^*$  is the forward voltage drop across the diodes). At small forward currents of 10 to 20  $\mu$ A the  $V^*$  is typically about 0.5 V for silicon  $p$ - $n$  junction diodes; thus  $2V^* \approx 1$  V. The characteristic resistance of the resonance loop is  $\rho \approx 650$   $\Omega$ . Then the set of four differential equations, convenient for numerical integration, is obtained:

$$\begin{cases} \frac{dx}{d\vartheta} = y, \\ \frac{dy}{d\vartheta} = kF(x) - x - by + cv, \\ \varepsilon \frac{dz}{d\vartheta} = v, \\ \mu \frac{dv}{d\vartheta} = ay - z - dv, \end{cases} \quad (4)$$

where the nonlinear function  $F(x)$  involving the current-voltage characteristic of the diodes is approximated by a three-segment piecewise linear function:

$$F(x) = \begin{cases} -0.5 & , \quad x < -0.5, \\ x & , \quad |x| < 0.5, \\ 0.5 & , \quad x > 0.5. \end{cases} \quad (5)$$

### Numerical results

Equations (3) have been integrated numerically using the Wolfram MATHEMATICA and FREEPASCAL computational software programs. The typical results for chaotic waveform and power spectrum are presented in Fig. 4 and Fig. 5, respectively.

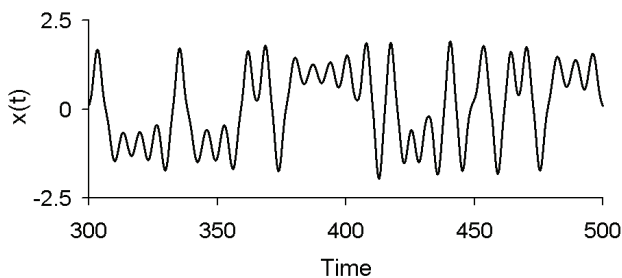


**Fig. 4.** Snapshot of chaotic waveform  $x(t)$  from Eqs. (3) with  $a = 0.6$ ,  $b = 0.1$ ,  $c = d = 0.15$ ,  $k = 2$ ,  $\varepsilon = 1.2$ ,  $\mu = 1$

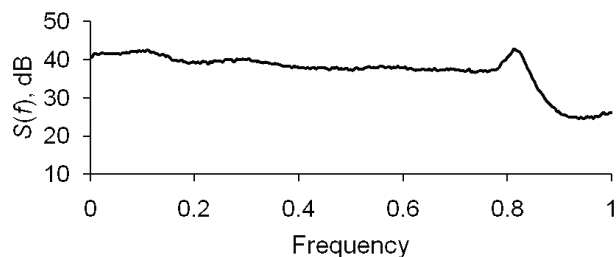


**Fig. 5.** Simulated power spectrum  $S(f)$  from the variable  $x(t)$  (parameters are the same as in Fig. 4)

### Conclusions

We have designed and built a novel Silva–Young type the fourth–order chaotic oscillator characterized by the spectral unevenness of less than 10 dB (Fig. 3a). Moreover, very simple second–order external resonant circuit  $L_3R_8C_3$  (Fig. 1) inserted in the output follower allows decreasing this value to less than 3 dB (Fig. 3b).

On one hand, the developed fourth–order oscillator can be considered as an extended version of the previously

proposed third–order chaotic oscillator [22] in the sense that its order is simply increased from three to four. On the other hand, the novel oscillator is similar from the structural point of view to the second–order nonautonomous Silva–Young circuit [15, 16]. The only difference of the suggested fourth–order circuit is that the *external* periodic driving oscillator in the original Silva–Young circuit is replaced with a passive *internal* second–order resonance circuit  $L_2R_5C_2$  (Fig. 1), inserted in the second positive feedback loop. Nevertheless, this replacement yields fairly flat power spectrum of the output signal with no peaks at the resonant frequencies.

### References

1. Special Issue on Chaotic Systems // Proceedings of the IEEE. – 1987. – Vol. 75. – No. 8.
2. **Chen G., Ueta T.** (eds.) Chaos in Circuits and Systems. – Singapore. – World Scientific Publishing Co, 2002.
3. **Namajūnas A., Tamaševičius A.** Modified Wien–Bridge Oscillator for Chaos // Electronics Letters, 1995. – Vol. 31. – No. 5. – P. 335–336.
4. **Namajūnas A., Tamaševičius A.** RC Chaotic Oscillator // Electronics and Electrical Engineering. – Kaunas: Technologija, 1996. – No. 1(5). – P. 40–42.
5. **Namajūnas A., Tamaševičius A.** Simple RC Chaotic Oscillator // Electronics Letters, 1996. – Vol. 32. – No. 11. – P. 945–946.
6. **Baziliauskas A., Krivickas R., Tamaševičius A.** Coupled Chaotic Colpitts Oscillators: Identical and Mismatched Cases // Nonlinear Dynamics, 2006. – V. 44. – No. 1–4. – P. 151–158.
7. **Tamaševičius A., Mykolaitis G., Bumelienė S., Baziliauskas A., Krivickas R., Lindberg E.** Chaotic Colpitts Oscillator for the Ultrahigh Frequency Range // Nonlinear Dynamics, 2006. – Vol. 44. – No. 1–4. – P. 159–165.
8. **Tamaševičius A., Namajūnas A., Čenys A.** Simple 4D Chaotic Oscillator // Electronics Letters, 1996. – Vol. 32. – No. 11. – P. 957–958.
9. **Tamaševičius A., Čenys A., Mykolaitis G., Namajūnas A., Lindberg E.** Hyperchaotic Oscillator with Gytrators // Electronics Letters, 1997. – Vol. 33. – No. 71. – P. 542–544.
10. **Mykolaitis G., Tamaševičius A., Bumelienė S., Baziliauskas A., Lindberg E.** Two–Stage Chaotic Colpitts Oscillator for the UHF Range // Electronics and Electrical Engineering. – Kaunas: Technologija, 2004. – No. 4(53). – P. 13–15.
11. **Bumelienė S., Tamaševičius A., Mykolaitis G., Baziliauskas A., Lindberg E.** Numerical Investigation and Experimental Demonstration of Chaos from Two–Stage Chaotic Colpitts Oscillator in the Ultrahigh Frequency Range // Nonlinear Dynamics, 2006. – Vol. 44. – No. 1–4. – P. 167–172.
12. **Čenys A., Tamaševičius A., Baziliauskas A., Krivickas R., Lindberg E.** Hyperchaos in Coupled Colpitts Oscillators // Chaos, Solitons & Fractals, 2003. – Vol. 17. – No. 2. – P. 349–353.
13. **Namajūnas A., Pyragas K., Tamaševičius A.** Analog Techniques for Modeling and Controlling the Mackey–Glass System // International Journal of Bifurcation and Chaos, 1997. – Vol. 7. – No. 4. – P. 957–962.
14. **Hilborn R. C.** Chaos and Nonlinear Dynamics: An Introduction for Scientists and Engineers. – Oxford University Press. – 2006.
15. **Silva C. P., Young A. M.** High Frequency Anharmonic Oscillator for the Generation of Broadband Deterministic Noise, 2000. – U.S. Patent No. 6,127,899.

16. **Silva C. P., Young A. M.** Implementing RF Broadband Chaotic Oscillators: Design Issues and Results // Proceedings of the IEEE International Symposium on Circuits and Systems. – IEEE, 1998. – Vol. 4. – P. 489–493.
17. **Kandangath A., Krishnamoorthy S., Lai Y.-C., Gaudet J. A.** Inducing Chaos in Electronic Circuits by Resonant Perturbations // IEEE Trans. Circuits and Systems–I, 2007. – Vol. 54. – P. 1109–1119.
18. **Tamaševičiūtė E., Tamaševičius A., Mykolaitis G., Bumelienė S., Lindberg E.** Analogue Electrical Circuit for Simulation of the Duffing–Holmes Equation // Nonlinear Analysis: Modelling and Control, 2008. – Vol. 13. – P. 241–252.
19. **Tamaševičius A., Tamaševičiūtė E., Mykolaitis G., Bumelienė S.** Switching from Stable to Unknown Unstable Steady States of Dynamical Systems // Physical Review E., 2008. – Vol. 78. – No. 2.
20. **Tamaševičius A., Tamaševičiūtė E., Pyragienė T., Mykolaitis G., Bumelienė S.** Extended Resonant Feedback Technique for Controlling Unstable Periodic Orbits of Chaotic System // Communications in Nonlinear Science and Numerical Simulation, 2009. – Vol. 78. – No. 12. – P. 4273–4279.
21. **Lindberg E., Tamaševičiūtė E., Mykolaitis G., Bumelienė S., Pyragienė T., Tamaševičius A., Kirvaitis R.** Autonomous Third–Order Duffing–Holmes Type Chaotic Oscillator // Proceedings of the 2009 European Conference on Circuit Theory and Design (ECCTD'09). – Antalya, Turkey, 2009. – P. 663–666.
22. **Tamaševičius A., Bumelienė S., Kirvaitis R., Mykolaitis G., Tamaševičiūtė E., Lindberg E.** Autonomous Duffing–Holmes Type Chaotic Oscillator // Electronics and Electrical Engineering. – Kaunas: Technologija, 2009. – No. 5(93). – P. 43–46.

Received 2011 02 06

Accepted after revision 2011 09 14

**E. Tamaseviciute, G. Mykolaitis, A. Tamasevicius. Autonomous Silva–Young Type Chaotic Oscillator with Flat Power Spectrum // Electronics and Electrical Engineering. – Kaunas: Technologija, 2011. – No. 9(115). – P. 109–112.**

A novel Silva–Young type fourth–order autonomous chaotic oscillator is described. In comparison with the original nonautonomous Silva–Young circuit it lacks the external periodic driving oscillator, but includes a passive internal second–order resonant LRC circuit, inserted in the positive feedback loop. In contrast to many other nonautonomous and autonomous chaotic oscillators, the suggested circuit exhibits fairly flat power spectrum of the output signal. Hardware experimental results and numerical results are presented. Good agreement between numerical and experimental results is observed. Ill. 5, bibl. 22 (in English; abstracts in English and Lithuanian).

**E. Tamaševičiūtė, G. Mykolaitis, A. Tamaševičius. Autonominis Silvos ir Youngo tipo chaotinis generatorius su plokščiuoju galios spektru // Elektronika ir elektrotechnika. – Kaunas: Technologija, 2011. – Nr. 9(115). – P. 109–112.**

Aprašomas naujas Silvos ir Youngo tipo ketvirtosios eilės chaotinių virpesių autogeneratorius. Skirtingai nuo originaliosios neautonominės Silvos ir Youngo grandinės, jame nėra išorinio periodinio žadinimo generatoriaus. Vietoj jo teigiamojo grįžtamojo ryšio kilpoje įtaisyta antrosios eilės rezonancinė LRC grandinė. Priešingai nei daugelyje kitų neautonominių ir autonominių chaotinių generatorių, pasiūlytoji grandinė pasižymi gana plokščiu išėjimo signalo galios spektru. Pateiktieji eksperimentinio tyrimo ir skaitinio modeliavimo rezultatai tarpusavyje gana gerai sutampa. Il. 5, bibl. 22 (anglų kalba; santraukos anglų ir lietuvių k.).